

# The speciation of Ni and Co in silicate melts from optical absorption spectra to 1500°C

Hans Keppler<sup>\*</sup>, Nicholas Bagdassarov<sup>1</sup>

*Bayerisches Geoinstitut, Universität Bayreuth, 95440 Bayreuth, Germany*

Received 22 July 1998; received in revised form 31 January 1999; accepted 31 January 1999

## Abstract

The optical absorption spectra of  $\text{Co}^{2+}$  and  $\text{Ni}^{2+}$  in haplogranitic glass and melt were measured from room temperature to 1500°C. For  $\text{Co}^{2+}$ , a continuous decrease of the intensity of all bands with increasing temperature is observed both below and above the glass transition. This is attributed to a decrease of extinction coefficients with temperature.  $\text{Co}^{2+}$  is in a distorted tetrahedral environment both in the melt and in the quenched glass. The decrease of extinction coefficients with temperature may be related to a reduction of tetrahedral distortion. At low temperatures, a small fraction of  $\text{Co}^{2+}$  may be octahedrally coordinated, but spectroscopic evidence is not conclusive.  $\text{Ni}^{2+}$  is mostly in a distorted octahedral environment in the glass. Up to the glass transition temperature, the extinction coefficients of the bands of octahedral  $\text{Ni}^{2+}$  decrease slightly; however, beyond the glass transition, the intensity of the octahedral bands decrease rapidly and above 1300°C, the optical spectra are dominated by a band due to tetrahedral  $\text{Ni}^{2+}$ , indicating a change of coordination with temperature. The equilibrium constant for the reaction  $\text{Ni}_{\text{octahedral}}^{2+} = \text{Ni}_{\text{tetrahedral}}^{2+}$  is estimated to be  $\ln K = 8.42 - 11.13 \text{ K/T}$ , corresponding to a reaction enthalpy of 92 kJ/mol. Preliminary measurements suggest that the speciation of  $\text{Ni}^{2+}$  and  $\text{Co}^{2+}$  in basaltic systems is similar to that observed in haplogranite. Our results imply that the partitioning of  $\text{Ni}^{2+}$  between minerals and silicate melts should depend more strongly on temperature than for  $\text{Co}^{2+}$  and most other trace elements. © 1999 Elsevier Science B.V. All rights reserved.

*Keywords:* Silicate melts; Glasses; Nickel; Cobalt; Optical spectroscopy

## 1. Introduction

During recent years, numerous studies have probed the speciation of silicate melts by direct spectroscopic measurements at high temperature (e.g., McMillan and Wolf, 1995). In many cases it

was found that the structure of the melt far above the glass transition temperature  $T_g$  can be quite different from the structure of the quenched glass. In particular, Raman spectroscopy has proved to be a very powerful tool to study the connectivity of silicate tetrahedra in melts at very high temperatures; complementary information on equilibria and exchange dynamics of various silicate species in the melt can be obtained by  $^{29}\text{Si}$  NMR methods (e.g., Stebbins, 1995). On the other hand, there are only relatively few studies on the environment of network-modifying ions in silicate melts above  $T_g$ . However, knowl-

<sup>\*</sup> Corresponding author. Fax: +49-921-553769; e-mail: hans.keppler@uni-bayreuth.de

<sup>1</sup> Present address: Institut für Meteorologie und Geophysik, Universität Frankfurt, Feldbergstr. 47, 60323 Frankfurt am Main, Germany.

edge of the structural environment of these ions in the melt is crucial for understanding trace element partitioning between silicate melts and minerals.

The transition metals cobalt and nickel have received considerable attention by geochemists, because their abundance in the upper mantle can be used to constrain models of core formation (e.g., Thibault and Walter, 1995). Together with iron, nickel is the main constituent of the core. Moreover, due to its strong partitioning into olivine (Hart and Davis, 1978), the abundance of nickel in basaltic melts is a sensitive indicator of olivine fractionation, both on a small scale as well as on the scale of a global magma ocean.

Data on the speciation of  $\text{Ni}^{2+}$  in silicate melts above  $T_g$  are essentially limited to the work of Farges and Brown (1996) who report X-ray absorption data in sodium disilicate melt to 1000°C. The speciation of  $\text{Ni}^{2+}$  in potassium borate glass and melt was studied by Lin and Angell (1984) using optical spectroscopy. No comparable data are available for  $\text{Co}^{2+}$  in silicate melts, but there are some high-temperature spectroscopic studies of  $\text{Co}^{2+}$  in nitrate and halide glasses (Barkatt and Angell, 1978; Michailov and Nemilov, 1981). In the present paper, we present optical absorption spectra of  $\text{Co}^{2+}$  and  $\text{Ni}^{2+}$  in aluminosilicate melts to 1500°C. The speciation models derived from these measurements will help to understand the partitioning of transition metals in magmatic processes.

## 2. Experimental methods

A haplogranitic glass with the composition of 40 wt.%  $\text{NaAlSi}_3\text{O}_8$ –35 wt.%  $\text{SiO}_2$ –25 wt.%  $\text{KAlSi}_3\text{O}_8$  was prepared by melting a stoichiometric mixture of reagent-grade  $\text{SiO}_2$ ,  $\text{Al}_2\text{O}_3$ ,  $\text{K}_2\text{CO}_3$  and  $\text{Na}_2\text{CO}_3$  in a platinum crucible. The glass was then ground up and mixed with 1 wt.%  $\text{CoO}$  or  $\text{NiO}$ , respectively. Previous work (Keppler, 1992) showed that the speciation of Ni and Co in glasses is independent of concentration in the range between 0.1 and 1 wt.% Co or Ni. Melting of the powder in a platinum crucible at 1600°C for 1 h and slowly cooling the crucible in air produced dark blue (Co) or brown (Ni), homogeneous glasses. The cooling rate in the range of the glass transition was about 1–2°C/min.

Glass cylinders with 1 mm diameter were drilled out of the massive chunks of glass using hollow diamond drills. The cylinders were cut to a thickness of 1 mm and polished on both sides. These cylinders were wrapped on the sides into platinum foil and mounted in a microscope heating stage of the type described by Zapunnyy et al. (1989). A type S thermocouple was directly attached to the glass cylinders.

The heating stage with the samples was placed on an infrared microscope coupled to a Bruker IFS 120 Fourier-transform spectrometer. This spectrometer contains a permanently aligned, Michelson-type interferometer. The optics of the microscope is all-reflecting with a 15-fold Cassegranian objective. To record the optical spectra at various temperatures, several hundred scans were accumulated with  $8\text{ cm}^{-1}$  resolution using a Xenon-arc source, a quartz-beamsplitter with dielectric coating and a Si-diode as detector. With this setup, the spectral range from about 9000 to 27000  $\text{cm}^{-1}$  is accessible, which is sufficient to monitor the speciation of  $\text{Co}^{2+}$  and  $\text{Ni}^{2+}$  in the silicate glass and melt.

Measurements were carried out from room temperature to 1500°C. The temperature was essentially limited by the capability of the heating stage and by the deformation of the sample surface at high temperature. This deformation often leads to a sample geometry that refracts the beam out of the optical axis of the microscope, so that insufficient intensity reaches the detector. Blackbody radiation emitted from the sample was not a problem, even at the highest temperature, since this radiation is unmodu-

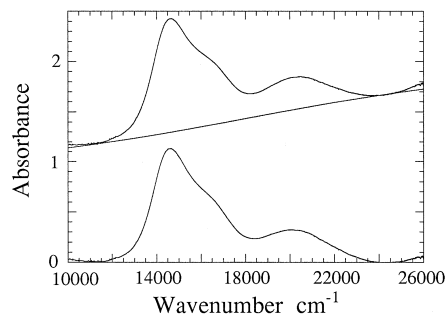


Fig. 1. Baseline correction of optical spectra. Shown are the raw data, the linear baseline, and the baseline-corrected spectrum of  $\text{Co}^{2+}$  in haplogranite melt at 1000°C. Sample thickness 1 mm, 1 wt.%  $\text{CoO}$ .

lated and in a Fourier-transform spectrometer, the spectrum is calculated from the modulated part of the radiation only. A detailed discussion of the technology used to acquire absorption spectra at high temperature can be found in (Keppler, 1996). After the heating cycle, samples were recovered and repolished. Spectra obtained from these samples were virtually indistinguishable from the spectra measured before the heating experiments.

A linear baseline correction was applied to all spectra measured at ambient conditions or at high temperature. The baseline was defined by the minima in absorption at low and high frequency, i.e., around 10,000 and 25,000  $\text{cm}^{-1}$ . An example for such a baseline correction is shown in Fig. 1.

### 3. Results

#### 3.1. Cobalt

Fig. 2 shows the baseline-corrected optical absorption spectrum of  $\text{Co}^{2+}$  in haplogranite glass at room temperature. The spectrum is very similar to that of  $\text{Co}^{2+}$  in albite glass (Keppler, 1992). Three band components centered around 15,000, 16,500, and 20,000  $\text{cm}^{-1}$  can clearly be distinguished. These bands are essentially due to crystal field transitions between the d-orbitals of  $\text{Co}^{2+}$  in a distorted tetrahedral environment. The individual bands are due to the spin-allowed transition  ${}^4\text{A}_2(\text{F}) \rightarrow {}^4\text{T}_1(\text{P})$ , combined with the two spin-forbidden transitions  ${}^4\text{A}_2(\text{F})$

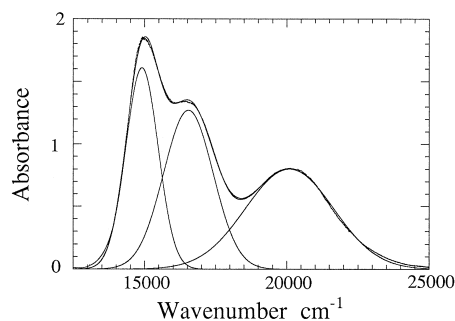


Fig. 2. Optical spectrum of  $\text{Co}^{2+}$  in haplogranite glass at 20°C, deconvoluted into three Gaussian components. Sample thickness 1 mm, 1 wt.% CoO. The positions of the individual band components are 14,908, 16,544, and 20,092  $\text{cm}^{-1}$ . For more information, see Table 1.

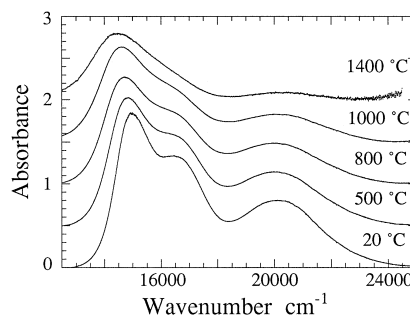


Fig. 3. Optical spectra of  $\text{Co}^{2+}$  in haplogranite glass and melt at selected temperatures. Sample thickness 1 mm, 1 wt.% CoO.

$\rightarrow {}^2\text{T}_1(\text{G})$ ,  ${}^2\text{E}_2(\text{G})$  and  ${}^4\text{A}_2(\text{F}) \rightarrow {}^2\text{T}_2(\text{G})$ . The spin-forbidden transitions are enhanced due to distortion; for further discussion of the spectra, see Keppler (1992).

Any absorption due to octahedral  $\text{Co}^{2+}$  would be expected to occur at higher frequency than for the tetrahedral species, with the main bands centered at or above 20,000  $\text{cm}^{-1}$  (e.g., Figgis, 1966). It cannot be ruled out that a small proportion of  $\text{Co}^{2+}$  is in an octahedral environment and that the corresponding bands are hidden below the 20,000  $\text{cm}^{-1}$  component of the tetrahedral spectrum. However, the fraction of octahedral  $\text{Co}^{2+}$  would have to be very small.

Fig. 3 shows some selected, baseline-corrected spectra of  $\text{Co}^{2+}$  in haplogranitic glass and melt to 1400°C. A number of changes are obvious with increasing temperature. The magnitude of absorption, i.e., the extinction coefficients of all bands decrease with temperature. This effect is particularly strong for the high-frequency band at 20,000  $\text{cm}^{-1}$ . At 1500°C, this band is not detectable anymore. Interestingly, the changes in the spectra start to occur far below the glass transition temperature, which should be around 600 to 800°C. At 500°C, for example, the intensity of the band responsible for the shoulder around 16,500  $\text{cm}^{-1}$  is already significantly reduced.

In order to quantify the changes occurring with temperature, the spectra were deconvoluted using three Gaussian functions as shown in Fig. 2. Position, width and intensity of the Gaussian components were allowed to vary freely without any constraints. Excellent fits with residual errors around 1% were achieved for all temperatures (Table 1). The individ-

Table 1  
Deconvolution of the optical spectra of  $\text{Co}^{2+}$  in haplogranite glass and melt to 1500°C

| Temperature (°C) | Frequency ( $\text{cm}^{-1}$ ) | Width ( $\text{cm}^{-1}$ ) | Intensity ( $\text{cm}^{-1}$ ) | Frequency ( $\text{cm}^{-1}$ ) | Width ( $\text{cm}^{-1}$ ) | Intensity ( $\text{cm}^{-1}$ ) | Frequency ( $\text{cm}^{-1}$ ) | Width ( $\text{cm}^{-1}$ ) | Intensity ( $\text{cm}^{-1}$ ) |
|------------------|--------------------------------|----------------------------|--------------------------------|--------------------------------|----------------------------|--------------------------------|--------------------------------|----------------------------|--------------------------------|
| 20               | 14,908                         | 1350                       | 2332                           | 16,544                         | 2033                       | 2756                           | 20,092                         | 3645                       | 3127                           |
| 250              | 14,828                         | 1411                       | 2247                           | 16,486                         | 2083                       | 2587                           | 20,063                         | 3695                       | 2890                           |
| 500              | 14,736                         | 1507                       | 2157                           | 16,430                         | 2110                       | 2281                           | 20,006                         | 3825                       | 2626                           |
| 600              | 14,700                         | 1564                       | 2126                           | 16,417                         | 2118                       | 2134                           | 19,978                         | 3845                       | 2468                           |
| 700              | 14,662                         | 1604                       | 2059                           | 16,394                         | 2141                       | 2004                           | 19,962                         | 3831                       | 2264                           |
| 800              | 14,615                         | 1657                       | 2004                           | 16,361                         | 2178                       | 1844                           | 19,977                         | 3800                       | 1982                           |
| 900              | 14,561                         | 1754                       | 2008                           | 16,332                         | 2212                       | 1610                           | 20,042                         | 3723                       | 1594                           |
| 1000             | 14,518                         | 1817                       | 1952                           | 16,294                         | 2227                       | 1404                           | 20,073                         | 3690                       | 1289                           |
| 1100             | 14,500                         | 1906                       | 1939                           | 16,302                         | 2179                       | 1153                           | 20,087                         | 3556                       | 972                            |
| 1200             | 14,479                         | 1986                       | 1904                           | 16,301                         | 2152                       | 961                            | 20,093                         | 3339                       | 696                            |
| 1300             | 14,461                         | 2037                       | 1782                           | 16,269                         | 2048                       | 723                            | 20,190                         | 2874                       | 363                            |
| 1400             | 14,471                         | 2194                       | 1777                           | 16,327                         | 1867                       | 491                            | 20,309                         | 2601                       | 206                            |
| 1500             | 14,476                         | 2609                       | 1692                           | 16,408                         | 1411                       | 178                            |                                |                            |                                |

Sample thickness 1 mm, 1 wt.%  $\text{CoO}$ . Spectra were deconvoluted into three Gaussian components. Residual errors are always around 1%. Width is full width at half height. Intensity refers to the integral intensity of individual band components.

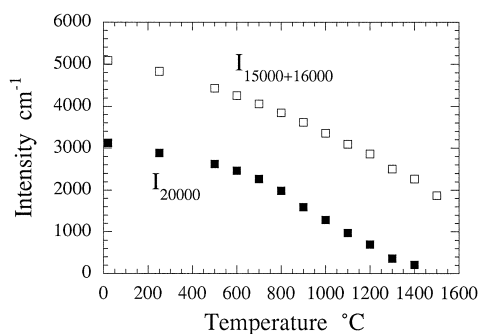


Fig. 4. Intensity of optical absorption bands of  $\text{Co}^{2+}$  in haplogranite glass and melt as function of temperature.

ual band positions show little variation with temperature. Intensities of Gaussian components are plotted as a function of temperature in Fig. 4. The intensities of the 15,000 and 16,500  $\text{cm}^{-1}$  bands have been added together, since the fitting procedure shows strong correlations between these components. The data in Fig. 4 do not suggest any change in  $\text{Co}^{2+}$  speciation at the glass transition temperature or in the melt phase. Rather, the decrease of extinction coefficients of all bands observed already in the glass continues smoothly across the glass transition around 700°C to temperatures up to 1500°C in the melt. Since a coordination change of  $\text{Co}^{2+}$  is highly unlikely to occur below the glass transition, this implies that the speciation also remains essentially unchanged in the melt, with  $\text{Co}^{2+}$  being tetrahedrally coordinated at all temperatures.

Optical absorption spectroscopy almost exclusively probes the first coordination shell around the transition metal ion. Accordingly, it is insensitive to changes at the glass transformation, if these changes occur far away from the  $\text{Co}^{2+}$  ion in the glass structure. It is therefore conceivable that rearrangements of the silicate network involving cleavage of Si–O–Si bonds are invisible in the optical spectra. This may be the reason why the glass transition has no obvious effect on the spectra of  $\text{Co}^{2+}$  in haplogranite, while it can be easily seen in the optical spectra of  $\text{Co}^{2+}$  doped into nitrate glasses (Barkatt and Angell, 1978).

The decrease in the extinction coefficients of all bands observed for  $\text{Co}^{2+}$  is probably related to a reduction of tetrahedral distortion with temperature. Normally, electronic transitions between d-orbitals

are forbidden for symmetry reasons, as they involve states with equal parity (e.g., Figgis, 1966). Crystal field bands can only be observed because there are several ways to lift this Laporte selection rule. If the transition metal ion is in a non-centrosymmetric environment, the d-orbitals interact with the surrounding electric fields and as a result of this, they are not strictly centrosymmetric anymore. In this case, transitions between different d-orbitals become allowed. The probability of a transition, i.e., the extinction coefficient will be the larger the stronger the coordination environment of the transition metal ion deviates from centrosymmetry. If the distortion of the coordination polyhedron around  $\text{Co}^{2+}$  decreased with temperature, absorption in the visible range should also decrease, as is observed. The decrease in absorption is particularly strong for the band around 20,000  $\text{cm}^{-1}$ . This band is assigned to the spin-forbidden transition  ${}^4\text{A}_2(\text{F}) \rightarrow {}^2\text{T}_2(\text{G})$  which normally should cause only very weak absorption. At room temperature, this band is probably intensified by interaction with a split component of the transition  ${}^4\text{A}_2(\text{F}) \rightarrow {}^4\text{T}_1(\text{P})$ , generated by low-symmetry distortion (Keppler, 1992). Accordingly, at high temperature, where tetrahedral distortion becomes negligible, the 20,000  $\text{cm}^{-1}$  band disappears.

### 3.2. Nickel

The spectrum of  $\text{Ni}^{2+}$  in haplogranite glass at room temperature is shown in Fig. 5. As with  $\text{Co}^{2+}$ , the spectrum is very similar to that measured in

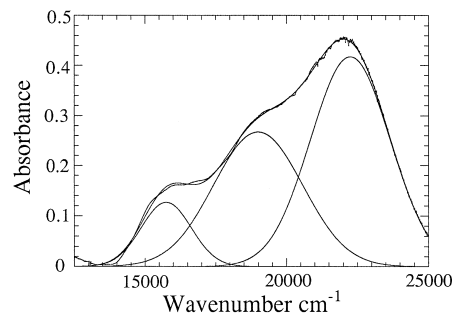


Fig. 5. Optical spectrum of  $\text{Ni}^{2+}$  in haplogranite glass at 20°C, deconvoluted into three Gaussian components. Sample thickness 1 mm, 1 wt.% NiO. The positions of the individual band components are 15,750, 18,998, and 22,250  $\text{cm}^{-1}$ . For more information, see Table 2.

albite glass (Keppler, 1992). Three bands are observed around 15,000, 19,000, and 22,000  $\text{cm}^{-1}$ . The two high-frequency components are due to the transition  ${}^3A_{2g}(F) \rightarrow {}^3T_{1g}(P)$  of  $\text{Ni}^{2+}$  in a distorted octahedral environment (Keppler, 1992). The band around 15,000  $\text{cm}^{-1}$  is at least partially due to the weak, spin-forbidden transition  ${}^3A_{2g}(F) \rightarrow {}^1E_g(D)$  of  $\text{Ni}^{2+}$  in this distorted octahedral site. However, tetrahedral  $\text{Ni}^{2+}$  would also absorb at this energy ( ${}^3T_1(F) \rightarrow {}^3T_1(P)$ ). It is therefore possible that a small amount of tetrahedral  $\text{Ni}^{2+}$  may be present in the glass and contribute to the absorption at 15,000  $\text{cm}^{-1}$ .

Based mainly on X-ray absorption measurements, it has been suggested that the distorted octahedral site of  $\text{Ni}^{2+}$  in silicate glasses would be more appropriately described as a five-coordinated site (Galoisy and Calas, 1993). However, this interpretation is not fully consistent with the optical absorption spectra (e.g., Keppler, 1992; Nowak and Keppler, 1998). Accordingly, we prefer a distorted octahedral model for this site. The distinction between distorted octahedral and fivefold coordination is not relevant for the following discussion of the speciation changes occurring in the melt at high temperature.

Fig. 6 shows some background-corrected high-temperature optical spectra of  $\text{Ni}^{2+}$  in haplogranite melt. Apparently, major speciation changes occur upon heating. Whereas the room temperature spectrum is dominated by the two bands of  $\text{Ni}^{2+}$  in a distorted octahedral site around 19,000 and 22,000  $\text{cm}^{-1}$ , these bands almost disappeared at 1300°C. At higher temperatures, they cannot be detected anymore at all, and the absorption spectrum is domi-

nated by the band close to 15,000  $\text{cm}^{-1}$ . At high temperatures, this band must be entirely due to tetrahedral  $\text{Ni}^{2+}$ , as the main bands of the distorted octahedral  $\text{Ni}^{2+}$  cannot be observed anymore.

To quantify the speciation changes, the spectra were deconvoluted using three Gaussian functions as shown in Fig. 5. As with  $\text{Co}^{2+}$ , position, width and intensity of the Gaussian components were allowed to vary freely without any constraints. Residual errors obtained in the fit were less than 0.5% at all temperatures (Table 2). The individual band positions show little variation with temperature. Intensities of Gaussian components are plotted as a function of temperature in Fig. 7; the intensities of the two bands of  $\text{Ni}^{2+}$  in distorted octahedral coordination at 19,000 and 22,000  $\text{cm}^{-1}$  were added together. Up to the glass transformation temperature around 700°C, the intensity due to distorted octahedral  $\text{Ni}^{2+}$  decreases only slightly, possibly again due to a reduction of polyhedral distortion, as with  $\text{Co}^{2+}$ . Part of this decrease may actually also be due to thermal expansion, which was not corrected for. Above  $T_g$ , however, the intensity drops of rapidly. The intensity of the band at 15,000  $\text{cm}^{-1}$ , where both distorted octahedral and tetrahedral  $\text{Ni}^{2+}$  absorb, remains roughly constant at all temperatures. These observations are all consistent with a conversion of distorted octahedral into tetrahedral  $\text{Ni}^{2+}$  with increasing temperature above  $T_g$ . This interpretation explains the decrease in intensity of the high-frequency bands. The 15,000  $\text{cm}^{-1}$  band remains roughly constant in intensity, probably because the increase in tetrahedral absorption in this range is approximately cancelled out by the decrease in octahedral absorption.

Below the glass transition temperature, the absorbance  $A$  of the 19,000 + 22,000  $\text{cm}^{-1}$  bands decreases linearly with temperature according to:

$$A/\text{cm}^{-1} = 2510.7 - 0.33987 T/^\circ\text{C}. \quad (1)$$

This equation is a linear fit through the data up to 600°C with  $R^2 = 0.983$ . It describes the decrease in optical absorption with temperature due to the intrinsic decrease of the extinction coefficients. If one assumes that this equation also approximately describes the intrinsic decrease of extinction coefficients above the glass transition, one can calculate the fraction of distorted octahedral  $\text{Ni}^{2+}$  at any

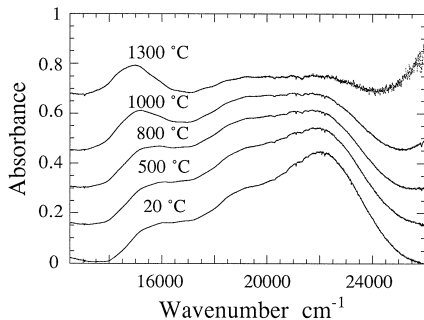


Fig. 6. Optical spectra of  $\text{Ni}^{2+}$  in haplogranite glass and melt at selected temperatures. Sample thickness 1 mm, 1 wt.% NiO.

Table 2  
Deconvolution of the optical spectra of Ni<sup>2+</sup> in haplogranite glass and melt to 1300°C

| Temperature (°C) | Frequency (cm <sup>-1</sup> ) | Width (cm <sup>-1</sup> ) | Intensity (cm <sup>-1</sup> ) | Frequency (cm <sup>-1</sup> ) | Width (cm <sup>-1</sup> ) | Intensity (cm <sup>-1</sup> ) | Frequency (cm <sup>-1</sup> ) | Width (cm <sup>-1</sup> ) | Intensity (cm <sup>-1</sup> ) |
|------------------|-------------------------------|---------------------------|-------------------------------|-------------------------------|---------------------------|-------------------------------|-------------------------------|---------------------------|-------------------------------|
| 20               | 15,750                        | 2080                      | 280                           | 18,998                        | 3678                      | 1048                          | 22,250                        | 3291                      | 1462                          |
| 250              | 15,670                        | 2022                      | 260                           | 19,191                        | 4176                      | 1247                          | 22,337                        | 3153                      | 1165                          |
| 500              | 15,598                        | 2050                      | 267                           | 19,317                        | 4517                      | 1414                          | 22,387                        | 3043                      | 939                           |
| 600              | 15,560                        | 2064                      | 271                           | 19,314                        | 4584                      | 1429                          | 22,388                        | 3039                      | 873                           |
| 700              | 15,542                        | 2035                      | 263                           | 19,362                        | 4609                      | 1390                          | 22,372                        | 2875                      | 728                           |
| 800              | 15,462                        | 2047                      | 274                           | 19,370                        | 4651                      | 1352                          | 22,361                        | 2791                      | 617                           |
| 900              | 15,293                        | 1996                      | 290                           | 19,449                        | 4795                      | 1293                          | 22,381                        | 2695                      | 480                           |
| 1000             | 15,179                        | 2015                      | 308                           | 19,489                        | 4703                      | 1092                          | 22,360                        | 2530                      | 363                           |
| 1100             | 15,093                        | 1937                      | 284                           | 19,576                        | 4538                      | 808                           | 22,361                        | 2424                      | 264                           |
| 1200             | 15,023                        | 1758                      | 224                           | 19,533                        | 3362                      | 329                           | 22,170                        | 2342                      | 208                           |
| 1300             | 14,838                        | 2015                      | 278                           | 19,248                        | 2256                      | 115                           | 21,938                        | 2790                      | 181                           |

Sample thickness is 1 mm, 1 wt.% NiO. Spectra were deconvoluted into three Gaussian components. Residual errors are always less than 0.5%. Width is full width at half height. Intensity refers to the integral intensity of individual band components.

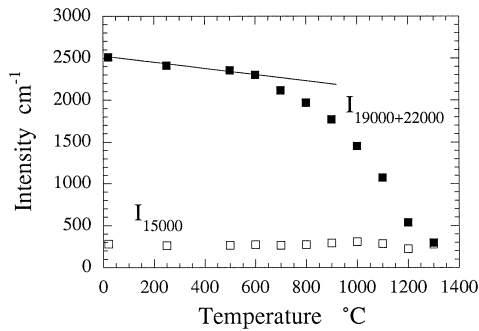


Fig. 7. Intensity of optical absorption bands of  $\text{Ni}^{2+}$  in haplogranite glass and melt as function of temperature.

temperature in a very simple way. This fraction is simply obtained by dividing the integral absorption of the 19,000 and 22,000  $\text{cm}^{-1}$  bands at any given temperature by the absorption predicted from Eq. (1). The fraction of tetrahedral  $\text{Ni}^{2+}$  is then given by difference:

$$\text{Ni}^{\text{IV}} = 1 - \text{Ni}^{\text{VI}}. \quad (2)$$

The results of this calculation are shown in Table 3. An implicit assumption in the calculation is that virtually all of the  $\text{Ni}^{2+}$  is in a distorted octahedral site in the glass below  $T_g$ . As noted above, the presence of a small amount of tetrahedral  $\text{Ni}^{2+}$  in the glass cannot be ruled out. This may cause a systematic error in the species calculation, which, however, should not exceed a few percent.

Table 3  
Coordination of  $\text{Ni}^{2+}$  in haplogranite melt

| Temperature (°C) | Octahedral intensity ( $\text{cm}^{-1}$ ) | Predicted intensity ( $\text{cm}^{-1}$ ) | Octahedral $\text{Ni}^{2+}$ ( $\text{Ni}^{\text{VI}}$ ) (%) | Tetrahedral $\text{Ni}^{2+}$ ( $\text{Ni}^{\text{IV}}$ ) (%) | $\ln(\text{Ni}^{\text{IV}}/\text{Ni}^{\text{VI}})$ |
|------------------|---|--|---|--|--|
| 20               | 2510                                      | 2504                                     | ≈ 100   | ≈ 0  |  |
| 250              | 2412                                      | 2426                                     | ≈ 100   | ≈ 0  |  |
| 500              | 2353                                      | 2341                                     | ≈ 100   | ≈ 0  |  |
| 600              | 2302                                      | 2307                                     | ≈ 100   | ≈ 0  |  |
| 700              | 2118                                      | 2273                                     | 93  | 7  | -2.62  |
| 800              | 1969                                      | 2239                                     | 88  | 12   | -1.98  |
| 900              | 1773                                      | 2205                                     | 80  | 20   | -1.41  |
| 1000             | 1455                                      | 2171                                     | 67  | 33   | -0.71  |
| 1100             | 1072                                      | 2137                                     | 50  | 50   | -0.01  |
| 1200             | 537                                       | 2103                                     | 25  | 75   | 1.07   |
| 1300             | 296                                       | 2069                                     | 14  | 86   | 1.79   |

Octahedral intensity is the sum of the intensities of the bands due to octahedral  $\text{Ni}^{2+}$  at 19,000 and 22,000  $\text{cm}^{-1}$ . Predicted intensity is the intensity of the octahedral bands as it would be expected if no speciation change occurred.

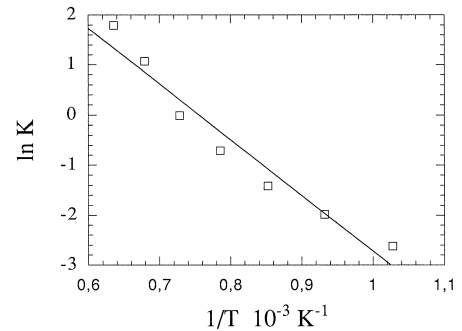


Fig. 8. Temperature dependence of the equilibrium constant for the conversion of distorted octahedral to tetrahedral  $\text{Ni}^{2+}$  in haplogranite melt.

The equilibrium between distorted octahedral and tetrahedral  $\text{Ni}^{2+}$  in the melt can be described by the equilibrium constant:

$$K = \text{Ni}^{\text{IV}}/\text{Ni}^{\text{VI}}. \quad (3)$$

Fig. 8 shows a plot of  $\ln K$  vs.  $1/T$ . The data can be fitted by the equation:

$$\ln K = 8.42 - 11.13 \cdot 10^3 \text{ K}/T \quad (4)$$

with  $R^2 = 0.95$ . This corresponds to a reaction enthalpy of  $\Delta H = 92 \text{ kJ/mol}$  for the conversion of distorted octahedral to tetrahedral  $\text{Ni}^{2+}$  in the haplogranite melt.

Optical absorption measurements similar to those described above for haplogranite were also carried out with a synthetic, iron-free basaltic melt. The composition was close to a natural tholeiite, but with



all Fe replaced by Mg. These experiments were somewhat hampered by the low viscosity of these melts which caused rapid crystallization around the glass transition and severe deformation of the sample surfaces at higher temperatures. Due to these problems, the spectra obtained at high temperature are somewhat unsatisfactory and will not be discussed in further detail. All measurements carried out so far are however consistent with a similar coordination change of  $\text{Ni}^{2+}$  occurring in basaltic melts as observed in haplogranite.  $\text{Co}^{2+}$  remains tetrahedrally coordinated at all temperatures studied.

## 4. Discussion

### 4.1. Comparison with other systems

The observation of a coordination change of  $\text{Ni}^{2+}$  in haplogranite melt at high temperature is in excellent agreement with predictions of Seward (1971) and with recent experimental work of Farges and Brown (1996). Farges and Brown investigated the environment of  $\text{Ni}^{2+}$  in sodium disilicate glass and melt by X-ray absorption spectroscopy and observed a decrease of the average coordination number in the melt phase, suggesting that  $\text{Ni}^{2+}$  is mostly in tetrahedral coordination at high temperature. A similar coordination change of  $\text{Ni}^{2+}$  from octahedral to tetrahedral with increasing temperature has been observed to occur in a wide variety of solvents, including potassium borate melt (Lin and Angell, 1984), alkali chloride melts (Boston and Smith, 1958) and hydrous solutions (Angell and Gruen, 1966; Lüdemann and Franck, 1967). The reaction enthalpies for the coordination change observed in these systems are usually smaller than the value found in the present study for haplogranite melt. For example,  $\Delta H$  is 44.4 kJ/mol in potassium borate melt, 38.9 kJ/mol in alkali chloride melts, but 92 kJ/mol for haplogranite. This difference is, however, easily understood if one considers that the haplogranite melt is a fully polymerized network of silicate tetrahedra and therefore, any coordination change will require a rearrangement of the Si–O bonds.

The behavior of  $\text{Ni}^{2+}$  is somewhat unusual if compared with other trace elements in natural magmatic systems. A similar temperature dependent

equilibrium between four- and five-coordinated species has been suggested for  $\text{Fe}^{2+}$  in silicate melts (Brown et al., 1995, and references therein). However,  $\text{Co}^{2+}$ , as pointed out above, does not change coordination in the melt phase or when going from the glass to the melt. George and Stebbins (1998) presented high-temperature NMR evidence suggesting that the environment of  $\text{Mg}^{2+}$  in silicate melt and glass is similar over a wide range of temperatures. In addition, it has been shown by EXAFS-measurements (Brown et al., 1995) that the environment of most high field strength ions in silicate melts and glasses is virtually independent of temperature. A possible exception may be titanium, where some changes with temperature have been suggested (Mysen and Neuville, 1995). According to these data, one should expect that the partitioning of most trace elements is rather insensitive to temperature, while there should be a considerable temperature dependence for nickel and possibly for a few other elements.

### 4.2. Partition coefficients

$\text{Ni}^{2+}$  is an ion with exceptionally large crystal field stabilization energies (CFSE), particularly in an octahedral field. It has been shown that the partition coefficients of such ions, particularly of  $\text{Ni}^{2+}$  and  $\text{Cr}^{3+}$ , can be quantitatively predicted by considerations of crystal field effects (Keppler, 1992; Malavergne et al., 1997). Moreover, spectroscopic data from high-pressure experiments have been successfully used to predict the pressure dependence of the metal/silicate melt partition coefficients of  $\text{Ni}^{2+}$  and  $\text{Co}^{2+}$  (Keppler and Rubie, 1993; Thibault and Walter, 1995). In an octahedral site, the CFSE of  $\text{Ni}^{2+}$  in various phases is in the range of 75 to 140 kJ/mol, while the CFSE in a tetrahedral site is usually around 40 kJ/mol (Burns, 1993). Therefore,  $\text{Ni}^{2+}$  should strongly prefer octahedral over tetrahedral sites. According to the data reported by Burns (1993), the difference between the CFSE in both sites, the so-called octahedral site preference energy (OSPE), is in the order of 35–100 kJ/mol, depending on the specific system considered. Interestingly, this is just the range of reaction enthalpies measured in various melts for the conversion of octahedral to tetrahedral  $\text{Ni}^{2+}$ , as noted above.

If  $\text{Ni}^{2+}$  moves from distorted octahedral into tetrahedral coordination in silicate melts at high temperatures, CFSE in the melt will be reduced and accordingly,  $\text{Ni}^{2+}$  should tend to become more compatible in minerals, unless this effect is cancelled out by entropy changes. For  $\text{Co}^{2+}$ , which always remains in a tetrahedral site, no such effect is expected. Accordingly, the relative fractionation of Ni and Co between a silicate melt and a mineral, such as olivine, should change with temperature in such a way that at high temperature the uptake of  $\text{Ni}^{2+}$  in olivine is more favoured. This behaviour was found by Holzheid et al. (1997) in a thermodynamic analysis of Ni and Co partitioning between silicate melts and olivine. According to Holzheid et al.,  $K_D^{\text{Ni}/\text{Co}}$  for olivine increases from 1.13 at 1100°C to 1.34 at 1600°C. Holzheid et al. also noted that the activity coefficient of  $\text{Ni}^{2+}$  in silicate melts is dependent on temperature, if solid NiO is used as a standard state, but temperature independent if referenced to liquid NiO. As noted above, available evidence from a wide range of different systems suggests that  $\text{Ni}^{2+}$  always changes its coordination environment in a liquid as a function of temperature. It is therefore conceivable that liquid NiO contains  $\text{Ni}^{2+}$  in a mixture of different coordination environments, similar to the situation in silicate melts, while solid NiO only contains octahedral  $\text{Ni}^{2+}$ . The independence of activity coefficients of  $\text{Ni}^{2+}$  in silicate melts, if referenced to liquid NiO, would then simply be a result of similar coordination geometries in both melts.

### Acknowledgements

We would like to thank Hubert Schultze for sample preparation and Anna Dietel for chemical analyses. Constructive reviews by Francois Farges and Bjoern Mysen are very much appreciated. [MB]

### References

- Angell, C.A., Gruen, D.M., 1966. Octahedral–tetrahedral coordination equilibria of nickel (II) and copper (II) in concentrated aqueous electrolyte solutions. *J. Am. Chem. Soc.* 88, 5192–5198.
- Barkatt, A., Angell, C.A., 1978. Use of structural probe ions for relaxation studies in glasses: 2. Temperature-jump and temperature-ramp studies of cobalt (II) in nitrate glasses. *J. Phys. Chem.* 82, 1972–1979.
- Boston, C.R., Smith, G.P., 1958. Visible and ultraviolet absorption spectra of  $\text{NiCl}_2$  dissolved in fused  $\text{LiCl-KCl}$  mixtures. *J. Phys. Chem.* 62, 409–414.
- Brown, G.E., Farges, F., Calas, G., 1995. X-ray scattering and X-ray spectroscopy studies of silicate melts. *Rev. Mineral.* 32, 317–410.
- Burns, R.G., 1993. Mineralogical applications of crystal field theory, 2nd edn. Cambridge Univ. Press.
- Farges, F., Brown, G.E. Jr., 1996. An empirical model for the anharmonic analysis of high-temperature XAFS spectra of oxide compounds with applications to the coordination environment of Ni in NiO,  $\gamma\text{-Ni}_2\text{SiO}_4$  and Ni-bearing Na-disilicate glass and melt. *Chem. Geol.* 128, 93–106.
- Figgis, B.N., 1966. Introduction to Ligand Fields. Wiley, New York.
- Galoisy, L., Calas, G., 1993. Structural environment of nickel in silicate glass/melt systems: Part I. Spectroscopic determination of coordination states. *Geochim. Cosmochim. Acta* 57, 3613–3626.
- George, A.M., Stebbins, J.F., 1998. Structure and dynamics of magnesium in silicate melts: a high-temperature  $^{25}\text{Mg}$  NMR study. *Am. Mineral.* 83, 1022–1029.
- Hart, S.R., Davis, K.E., 1978. Nickel partitioning between olivine and silicate melt. *Earth Planet. Sci. Lett.* 40, 203–219.
- Holzheid, A., Palme, H., Chakraborty, S., 1997. The activities of NiO, CoO and FeO in silicate melts. *Chem. Geol.* 139, 21–38.
- Keppler, H., 1992. Crystal field spectra and geochemistry of transition metal ions in silicate melts and glasses. *Am. Mineral.* 77, 62–75.
- Keppler, H., 1996. The investigation of phase transitions by electronic absorption spectroscopy. *Phys. Chem. Miner.* 23, 288–296.
- Keppler, H., Rubie, D.C., 1993. Pressure-induced coordination changes of transition metal ions in silicate melts. *Nature* 364, 54–56.
- Lin, T.C., Angell, C.A., 1984. Electronic spectra and coordination of  $\text{Ni}^{2+}$  in potassium borate glass and melt to 1000°C. *Commun. Am. Ceram. Soc.* 1984, 33–34.
- Lüdemann, H.D., Franck, E.U., 1967. Absorptionsspektren bei hohen Drücken und Temperaturen: I. Wässrige Co(II) und Ni(II)-halogenid-Lösungen bis zu 500°C und 6 kbar. *Ber. Bunsenges. Phys. Chem.* 71, 455–460.
- Malavergne, V., Guyot, F., Wang, Y., Martinez, I., 1997. Partitioning of nickel, cobalt and manganese between silicate perovskite and periclase: a test of crystal field theory at high pressure. *Earth Planet. Sci. Lett.* 146, 499–509.
- McMillan, P.F., Wolf, G.H., 1995. Vibrational spectroscopy of silicate liquids. *Rev. Mineral.* 32, 247–315.
- Michailov, V.V., Nemilov, S.V., 1981. Spectral study of  $\text{Co}^{2+}$  in halide-bearing glass-forming matrices during the transition from solid to liquid state. *Fizika I Chimia Stekla* 7, 440–450, in Russian.
- Mysen, B.O., Neuville, D., 1995. Effect of temperature and  $\text{TiO}_2$  content on the structure of  $\text{Na}_2\text{Si}_2\text{O}_5\text{-Na}_2\text{Ti}_2\text{O}_5$  melts and glasses. *Geochim. Cosmochim. Acta* 59, 325–342.

- Nowak, M., Keppler, H., 1998. The influence of water on the environment of transition metals in silicate glasses. *Am. Mineral.* 83, 43–50.
- Seward, T.M., 1971. The distribution of transition elements in the system  $\text{CaMgSi}_2\text{O}_6\text{--Na}_2\text{Si}_2\text{O}_5\text{--H}_2\text{O}$  at 1000 bars pressure. *Chem. Geol.* 7, 73–95.
- Stebbins, J.F., 1995. Dynamics and structure of silicate and oxide melts: nuclear magnetic resonance studies. *Rev. Mineral.* 32, 191–246.
- Thibault, Y., Walter, M.J., 1995. The influence of pressure and temperature on the metal-silicate partition coefficients of nickel and cobalt in a model C1 chondrite and implications for metal segregation in a deep magma ocean. *Geochim. Cosmochim. Acta* 59, 991–1002.
- Zapunnyy, S.A., Sobolev, A.V., Bogdanov, A.A., Slutsky, A.B., Dmitriev, L.V., Kunin, L.L., 1989. An apparatus for high-temperature optical research with controlled oxygen fugacity. *Geochem. Int.* 26 (2), 120–128.